International Journal of Nanoelectronics and Materials
Volume 13 (Special Issue) Dec 2020 (173-192)

Curcumin Adsorption on Carbon Microparticles: Synthesis from Soursop (AnnonaMuricata L.) Peel Waste, Adsorption Isotherms and Thermodynamic and Adsorption Mechanism

Asep Bayu Dani Nandiyanto[1*], Zulfa Fathi Arinalhaq[1], Salma Rahmadianti[1], Mauseni Wantika Dewi[1], Yulian Putri Chandra Rizky[1], Aulia Maulidina[1], Sri Anggraeni[1], Muhammad Roil Bilad[2], Jumril Yunas[3]

[1]*Fakultas Pendidikan Matematika dan Ilmu Pengetahuan Alam, Universitas Pendidikan Indonesia, Jl. Dr. Setiabudi No. 229, Bandung 40154, Indonesia.*
[2]*Departement of Chemical Engineering, Universiti Teknologi Petronas, Malaysia.*
[3]*Institute of Micro Electronics and Nanotechnology, Universiti Kebangsaan Malaysia, Malaysia.*

ABSTRACT

The aims of this study was to evaluate adsorption isotherm of carbon microparticles prepared from calcination of soursop (Annona Muricata L.) peel waste (at temperature of 250 ℃). Adsorption test was done by mixing the prepared carbon microparticles (with sizes of 74, 250, and 500 μm) and curcumin (extracted from Indonesian local turmeric) in an aqueous solution at a constant pH, room temperature and pressure, and in the batch-typed adsorption reactor. Experimental results were then compared with the standard isotherm models, i.e., Langmuir, Temkin, Freundlich, Dubinin-Radushkevich, Flory-Huggins, Fowler–Guggenheim, and Hill-de Boer adsorption models. The results showed that particle size is very important to predict the adsorption process, therefore it is very important to have a homogeneous particle distribution (size and shape) to determine the adsorption properties. The data of regression value from the adsorption analysis indicated that the best fit isotherm models sequentially followed Hill-de Boer > Fowler > Flory > Temkin> Langmuir > Dubinin-Radushkevich > Freundlich. The adsorption process takes place on a multilayer surface, and the adsorbent-adsorbate interaction is a physical adsorption (which confirmed and is good agreement with the results from Hill-de Boer models and suitable with Freundlich, Temkin, and Dubinin-Radushkevich). Adsorption is carried out at different locations energetically under endothermic processes. The Gibbs free energy calculated is negative for all models, informing that the adsorption process is done spontaneously. This study demonstrates the useful process for producing carbon microparticles from soursop peel, giving good alternative for further development of carbon material from domestic waste.

Keywords: Adsorption isotherm, Carbon, Curcumin, Particle size, Soursop Peel.

1. INTRODUCTION

Carbon is the second most abundant element in the earth's crust after oxygen. Carbon is found in nature in three allotropic forms: amorphous, graphite, and diamond. All allotropes of carbon are solid under normal conditions, but graphite is the most thermodynamically stable allotrope instead of others[1].

Carbon is a material that has a variety of morphologies, including: colloidal carbon, nanotubes, fullerenese, graphite, graphene, colloidal sphere, nanofiber, porous carbon, nanowire, and activated carbon[2].

Carbon particles have attracted attentions of many scientists since they have the potential to be widely applied as adsorbents, catalysts, gas separation materials, drug delivery systems, and

*Corresponding Author: *nandiyanto@upi.edu*

energy storage materials. Furthermore, the main application of carbon particles relates to environmental protection and technological development. Carbon particles have high surface area, porous structure, narrow pore size distribution, high pore volume, low density, as well as chemically and thermally stable[3]. These unique characters make carbon an ideal candidate for adsorbents, enabling it to solve several issues such as environmental problems.

The consequence of the unique structures and properties of carbon material causes it be developed and applied in various fields. However, the use of high amounts of carbon still has limitations due to the high preparation costs, the low production yields, and the sophisticated equipment used. Therefore, the development of carbon-based materials functionally received a lot of attention because it has the capability of large-scale production at low cost. Several studies have shown that carbon can be made from a large number of readily available raw materials in an easy and cheap way, such as agricultural byproducts: Paulownia woods[4], tobacco residues[5], corncobs[6], coconut shells[7], mango seeds[8], cassava peels[9], pineapple peels[10], pumpkin seeds[11], solid palm shells[12], and palm kernel shells[13], as well as rice husks and rice straws[14-16]. From the precursor raw materials in agriculture, carbon is produced through the carbonization process. Although many studies have shown the successful carbon fabrication, the evaluation of carbon particles, especially those obtained from soursop shells for wider use (i.e. as an adsorbent) has not been widely studied.

This study aimed to investigate and evaluate the adsorption isotherm of carbon particles from soursop peel (*AnnonaMuricata L.*). Even though many researchers were working on the use of soursop peel for transforming them into adsorbent, our novelties are:

i. While other reports used hazardous chemicals, our research did not use hazardous chemicals so that it is environmentally friendly. Our method did not need additional chemicals since the carbon itself can be directly obtained from calcination of soursop peel waste.
ii. Most reports discussed about the successful synthesis and adsorption process, but less reports presented the adsorption isotherm.
iii. Less reports showed the use of soursop peel waste. In fact, soursop is one of the most product commodities in Indonesia. The commodity production of soursop in Indonesia was able to produce more than 15,000 tonnes per year[17, 18]. Then, since soursop is consumed without peel and the peels were disposed directly, the peel can create big problems for environment.

This study evaluated the conversion of soursop (*Annona Muricata L.*) peel waste into valuable materials (as a carbon microparticles as an adsorbent) and assessed the adsorption isotherm of the prepared carbon microparticles for adsorbing curcumin. In this study, soursop peel was used because it was not used properly (it became only household waste). Natural polymer components present in soursop skin (i.e., cellulose, lignin, and hemicellulose) can potentially be easily converted into carbon. The carbonization process uses high temperatures in order to break down the polymer structure of the biomass and release most of the non-carbon elements, especially oxygen, hydrogen, and nitrogen in the form of liquid and gas, leaving a carbon component in the final product[19]. The chemical structure of soursop peel contains mesoporousorganic component. Calcining the mesoporous organic can create mesoporous carbon material. Indeed, it can give functions to capture some materials/chemicals.

To analyze the adsorption ability of the prepared carbon microparticles, this study used curcumin as a model adsorbate[20]. The adsorption process was done in batch method under ambient temperature and constant pressure as well as constant pH. Experimental data obtained from the equilibrium studies were then fitted and compared to the standard isotherm models, i.e., Langmuir, Temkin, Freundlich, Dubinin-Radushkevich, Flory-Huggins, Fowler– Guggenheim, and Hill-de Boer adsorption models.

1.1 Adsorption Isotherm Models Used in this Study

This study used seven isotherm models adsorption such as Langmuir, Freundlich, Temkin, Dubinin-Radushkevich, Flory-Huggins[21], Fowler-Guggenheim[22], and Hill-de Boer[21] isotherm models for providing correlations for getting adsorption parameters.

1.1.1 Adsorption Efficiency

The adsorption efficiency (η) is measured using

$$\eta = \left(\frac{C_o - C_e}{C_o} \right) \times 100\% \tag{1}$$

where C_o is the initial concentration of adsorbate (mg/L). C_e is the concentration of adsorbate equilibrium (mg/L).

1.1.2 Langmuir Isotherm

The Langmuir adsorption isotherm model (Figure 1(a)) is based on several assumptions:

(i) the adsorption process occurs in a single layer (monolayer),
(ii) the process only takes place at specific homogeneous sites,
(iii) there is no molecular interaction between active sites,
(iv) all active sides can absorb only one type of atom or molecule.

The Langmuir equation is expressed as follows:

$$\frac{1}{Q_e} = \frac{1}{Q_{\max} K_L} \frac{1}{C_e} + \frac{1}{Q_{\max}} \tag{2}$$

C_e is the adsorbate equilibrium concentration (mg/L), K_L is the Langmuir adsorption constant, Q_e is the amount of adsorbed adsorbate molecules per gram of adsorbent (mg/g), and Q_{max} is the capacity of the adsorbent monolayer (mg/g).

Above equation is the used to get the separation factor (R_L) as a dimensionless constant, which can be calculated using following equation:

$$R_L = \frac{1}{1 + K_L C_e} \tag{3}$$

R_L value is used to classify what phenomena happen during the adsorption process:

(i) $R_L > 1$ shows the unfavorable adsorption process (adsorption is possible, but mostly desorption occurs).
(ii) $R_L = 1$ describes the linear adsorption process (the dependence of adsorbed amount and concentration is a straight line).
(iii) $R_L = 0$ explains the irreversible adsorption process (adsorption process is too strong).
(iv) $0 < R_L < 1$ is the favorable adsorption process (normal adsorption process).

1.1.3 Freundlich Isotherm

The Freundlich adsorption isotherm model (**Figure 1(b)**) states that the pores formed in the adsorbent are heterogeneous; thus, the adsorbed ions form a multilayer layer on the surface layer of the adsorbent. This model also states that active sites have different adsorption energies, sites that have the largest adsorption energy will be filled initially. The Freundlich equation can be written as follows:

$$\log Q_e = \log k_f + \frac{1}{n}\log C_e \tag{4}$$

Where k_f is the Freundlich constant, and n is the value indicating the degree of linearity between the adsorbate solution and the adsorption process. The value of n has a meaning in the following:

(i) $n = 1$ means the linear adsorption process (the adsorption process depends on the amount and concentration of adsorbate on the adsorbent).
(ii) $n < 1$ means the involvement of a chemical adsorption.
(iii) $n > 1$ is the physical adsorption process.
(iv) $0 < 1/n < 1$ is the favorable adsorption process (normal adsorption process).
(v) $1/n > 1$ is the cooperative adsorption (adsorbates at one site of the adsorbent affecting different binding sites on the same adsorbent) (see **Figure 1 (b)**).

1.1.4 Temkin Isotherm

The Temkin model describes explicitly

(i) the presence of adsorbent-adsorbate,
(ii) the heat interactions the adsorption (temperature function) of all adsorbate molecules in the layer will decrease linearly,
(iii) the uniform distribution of binding energy.

The model is given by:

$$q_e = \beta_T \ln A_T + \beta_T \ln C_e \tag{5}$$

Where A_T is the binding equilibrium constant, β_T is the adsorption heat constant, and T is the absolute temperature. If β_T is smaller than 8 kJ/mol, the adsorption process occurs physically.

1.1.5 Dubinin-Radushkevich Isotherm

The Dubinin-Radushkevich model is usually used to estimate heterogeneity and free energy of adsorption. The Dubinin-Radushkevich model can be described as follows:

$$\ln q_e = \ln q_s - (\beta\varepsilon)^2 \tag{6}$$

Where q_s refers to the saturation capacity of theoretical isotherms, β is the Dubinin-Radushkevich isotherm constant, and ε is the Polanyi potential (J/mol). To solve the constants, the following equations are used:

$$\varepsilon = RT\ln\left[1+\frac{1}{C_e}\right] \tag{7}$$

$$E = \frac{1}{\sqrt{2\beta}} \tag{8}$$

Where E is the adsorbate energy per molecule as the energy needed to remove molecules from the surface. The equation describes:

(i) E< 8 kJ/mol is the physical adsorption.
(ii) 8 <E< 168 kJ/mol is the chemical adsorption.

1.1.6 Hill-de Boer isotherm

The Hill–de Boer isotherm model explains aboutmobile adsorption and lateral interaction among adsorbed molecules[21]. The model is approximated using

$$K_1.Ce = \frac{\theta}{1-\theta}\exp\left(\frac{\theta}{1-\theta} - \frac{K_2\theta}{RT}\right) \tag{9}$$

where K_1 is the Hill–de Boer constant (L/mg) and K_2 is the energetic constant of the interaction between adsorbed molecules (kJ/mol).

(i) K_2 > 0 kJ/mol is the attraction between adsorbed molecules.
(ii) K_2 < 0 kJ/mol is the repulsion between adsorbed molecules.
(iii) K_2 = 0 kJ/mol is no interaction between adsorbed molecules.

1.1.7 Fowler-Gunggenheim Isotherm

The Fowler–Guggenheim takes the lateral interaction of the adsorbed molecules during the adsorption process. The model is one of the simplest correlations allowing for the prediction in the lateral interaction between adsorbates[21]. This model is explicitly explained:

$$K_{FG}.C_e = \frac{\theta}{1-\theta}\exp\left(\frac{2.\theta.W}{R.T}\right) \tag{10}$$

Where K_{FG} is the Fowler–Guggenheim equilibrium constant (L/mg). W is the interaction energy between adsorbed molecules (kJ/mol), in which the value of W correlates with the heat of adsorption. The heat varies linearly with loading adsorbed molecules on the surface of adsorbent.

(i) W > 0 kJ/mol is the attraction between adsorbed molecules, and the existence of exothermic processes.
(ii) W < 0 kJ/mol is the repulsion between adsorbed molecules, and the existence of endothermic processes.
(iii) W = 0 kJ/mol is no interaction between adsorbed molecules.

1.1.8 Flory-Huggins Isotherm

The Flory-Huggins isotherm model is occasionally used for understanding degree of surface coverage characteristics of adsorbate onto surface of adsorbent. This model expresses the feasibility and spontaneous phenomena in the adsorption process[22]. The equation of Flory-Huggins isotherm is presented:

$$\frac{\theta}{C_O} = K_{FH}(1-\theta)^{nFH} \tag{11}$$

Where *nFH* is the number of adsorbate molecules occupying on the sorption sites on the surface of adsorbent. K_{FH} is the equilibrium Flory-Huggins constant.

1.1.9 Gibbs Free Energy

This energy is used for predicting the type of energy happening during the adsorption process[23]. The Gibbs free energy (ΔGf) predicts the spontaneity of the adsorption process, which is estimated using:

$$\Delta Gf \approx -RT \ln K_X \tag{12}$$

Where K_X is the adsorption constant based on isotherm models, such as K_L, K_f, K_2, K_{FG}, and K_{FH}. The ΔGf defines:

(i) ΔGf > 0 kJ/mol is the non-spontaneous adsorption.
(ii) ΔGf < 0 kJ/mol is the spontaneous adsorption.

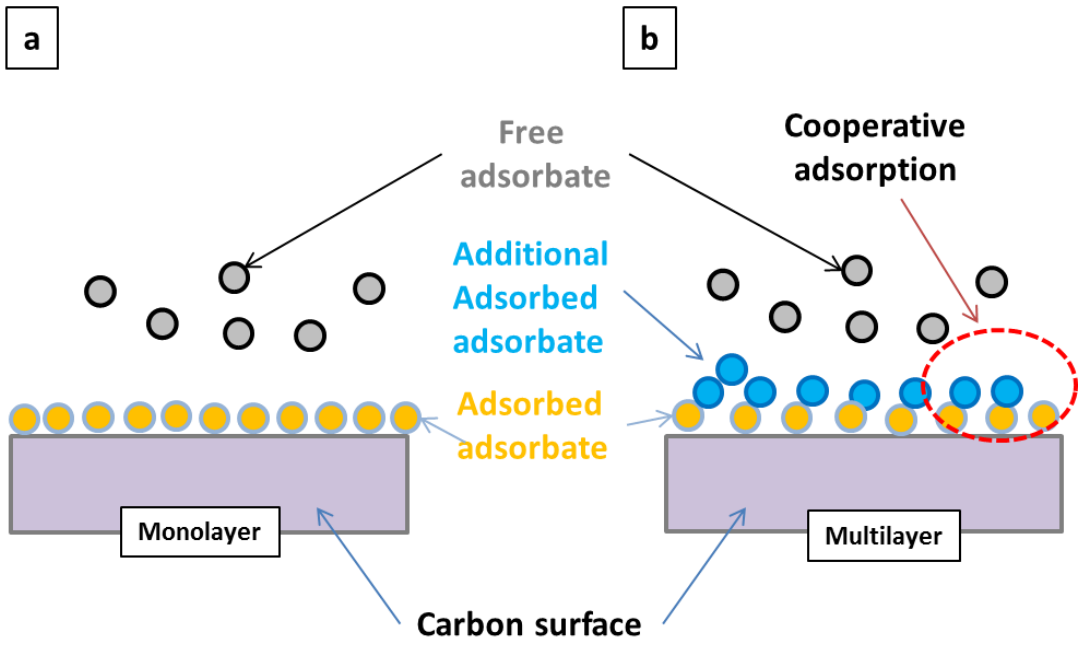

Figure 1. Adsorption Model: (a) Monolayer and (b) Multilayer.

2. MATERIAL AND METHODS

Preparation of carbon microparticles was done by conducting calcination to soursop (*AnnonaMuricata L.*) peel waste. The soursop peel waste was obtained from juice industries in Bandung, Indonesia. Prior to using as the carbon source, soursop peel was cleaned, washed, dried, skinned, and grounded using a saw-milling process. Detailed information for the saw-milling process is reported in our previous studies[24]. In short, the batch-typed saw-milling apparatus consists of a cylinder polytetrafluoroethylene milling vial (inner diameter = 7 cm; inner height = 10 cm), a single stainless steel blade unit (attached in the center bottom of the vial) with four 3-cm length jigsaw blades. The process was done at 18,000 rpm for 5 minutes for

each milling, and each milling was followed by manual mixing (using a metal spoon). To get a homogenous milling process, the milling was done five times for each sample. The saw-milling process is one of the popular method in making size-reduction material, such as dry-milling banana peels[25].

Detailed experimental procedure for preparing carbon microparticles are in the following: 500 g of soursop skin was cleaned, cut into small pieces, carbonized for 3 hours at 275°C. Then, the carbonization results were milled using the saw-milling apparatus to get powder form. The saw-milled product was then put into a test sieve apparatus (PT Rumah Publikasi Indonesia, Indonesia; hole sizes of 48, 55, 74, 100, 125, 250, 500, 1000, and 2000 μm) to separate the particle size. Then, the carbon particles were re-cleaned from their impurities by distilled water using a centrifugation (11000 rpm for 5 minutes) repeatedly. Carbon that was undergone centrifugation process was dried in the electrical oven for 2 hours at 80°C.

The adsorption isotherm test was conducted by mixing 0.05 g of the prepared carbon microparticles with specific sizes (i.e. 74, 250 and 500 μm) into 100 mL of curcumin solution (concentration of 20, 30, and 50 ppm; which was extracted using our previous method from Indonesian local turmeric (Curcuma Longa L.) obtained from local market in Bandung, Indonesia) in a batch-type adsorption apparatus (a 400-mL borosilicate batch glass having dimensions of 8 and 10 cm for diameter and height, respectively; equipped with a magnetic stirrer (1000 rpm)) for 20 minutes at room temperature and pressure. Adsorption process was done in the close system to ensure no light and no oxidation since curcumin is reactive. The adsorption profile was obtained by taking an aliquot (2-3 mL) in every 5 minutes from the adsorption apparatus, putting into the syringe filter (pore size of 220 nm), measuring the absorbance using a Visible Spectroscope (Model 7205; JENWAY; Cole-Parner; AS; at wavenumber of between 200 and 600 nm), plotting and normalizing the spectroscope results, and calculating using the Beer law analysis. The obtained data (concentration versus time) based on the Beer Law was then plotted and compared with the standard adsorption isotherm models: Langmuir, Freundlich, Temkin, Dubinin-Radushkevich, Flory-Huggins, Fowler– Guggenheim, and Hill-de Boer isotherm models.

3. RESULTS AND DISCUSSION

3.1 Physicochemical Properties of the Carbon Microparticles

Figure 2a showed the digital microscope image of carbon particles from soursop peel waste. The carbon material from soursop peel presented a heterogeneous surface with agglomerate particles. Figure 2b is the particle size analysis based on the digital microscope image to confirm the particle size distribution. Carbon particle size obtained from the sieve test results ranged from 48 to 2000 μm (see Figure 2b). The most fractions in sizes are 74, 250, and 500 μm. The main size of carbon particles is based on the highest percentage of mass distribution of each fraction.

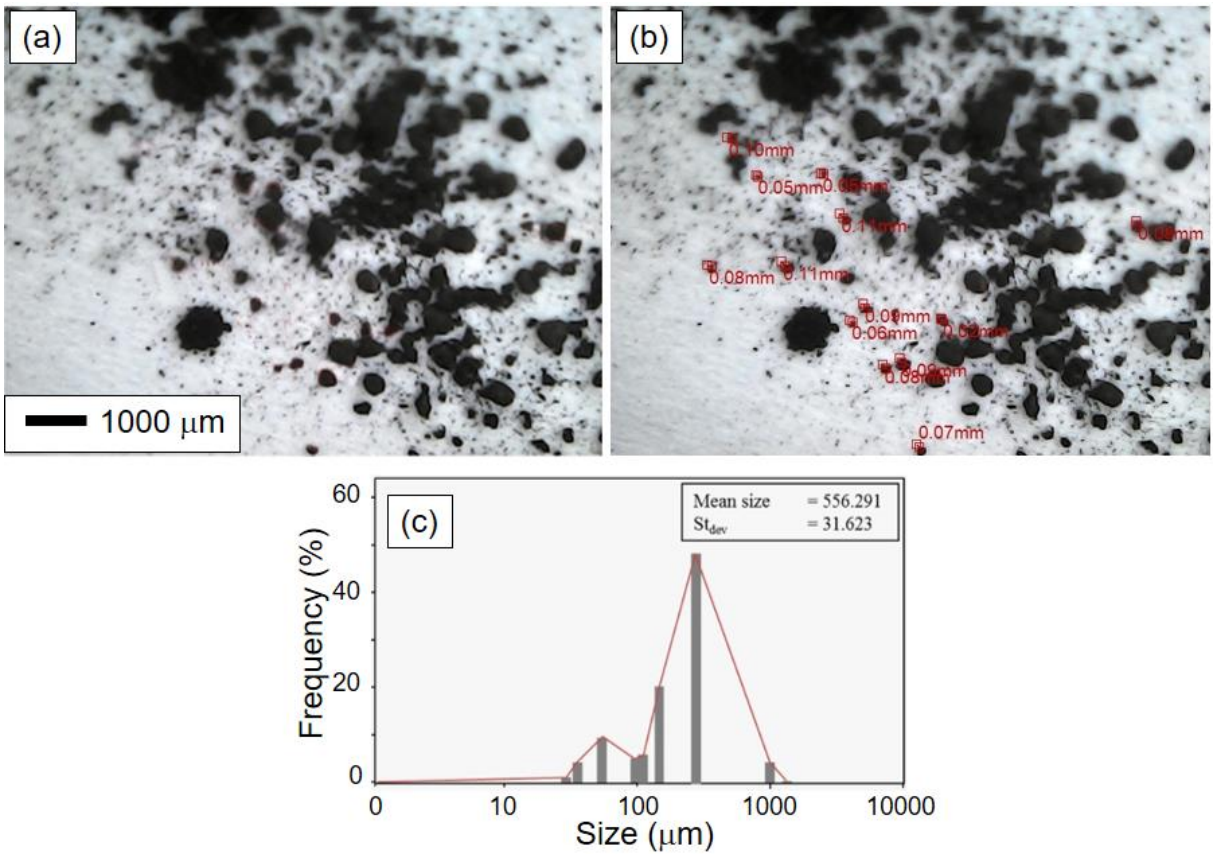

Figure 2. Photograph Image of Carbon Particle (a), Particle Size Analysis (b), and Particle Size Distribution Based on Sieve Test Measurement (c).

3.2 Adsorption Characteristics of Carbon Microparticles based on Isotherm Models

Figure 3 presents the correlation between efficiency and concentration of adsorbate under various sizes of carbon microparticles as adsorbent. All data agreed that the efficiency in adsorbing molecules depended on the particle sizes. The regression results from the data have almost identical gradient, but the intercept was different. Different values of intercepts are due to the effect of surface area on the adsorbent, in which smaller adsorbent sizes have larger surface area. To investigate the model of adsorption, experimental data were analyzed by a regression analysis to fit the linearized expression of mathematical models. The experimental values based on the plotting some parameters are reconstituted (using plot equations in Table 1). Experimental results (as points) and the theoretical calculated results (as lines) were plotted as presented in Figures 2-10. Linear correlation coefficients (R^2) are then used to show the compatibility of correlation curves between experimental data and linearized forms of the isotherm models. The plotting analysis can also derive several parameters in the adsorption process and predict what phenomena happening during the adsorption process. Parameters obtained from the plotting analysis is presented in Table 2.

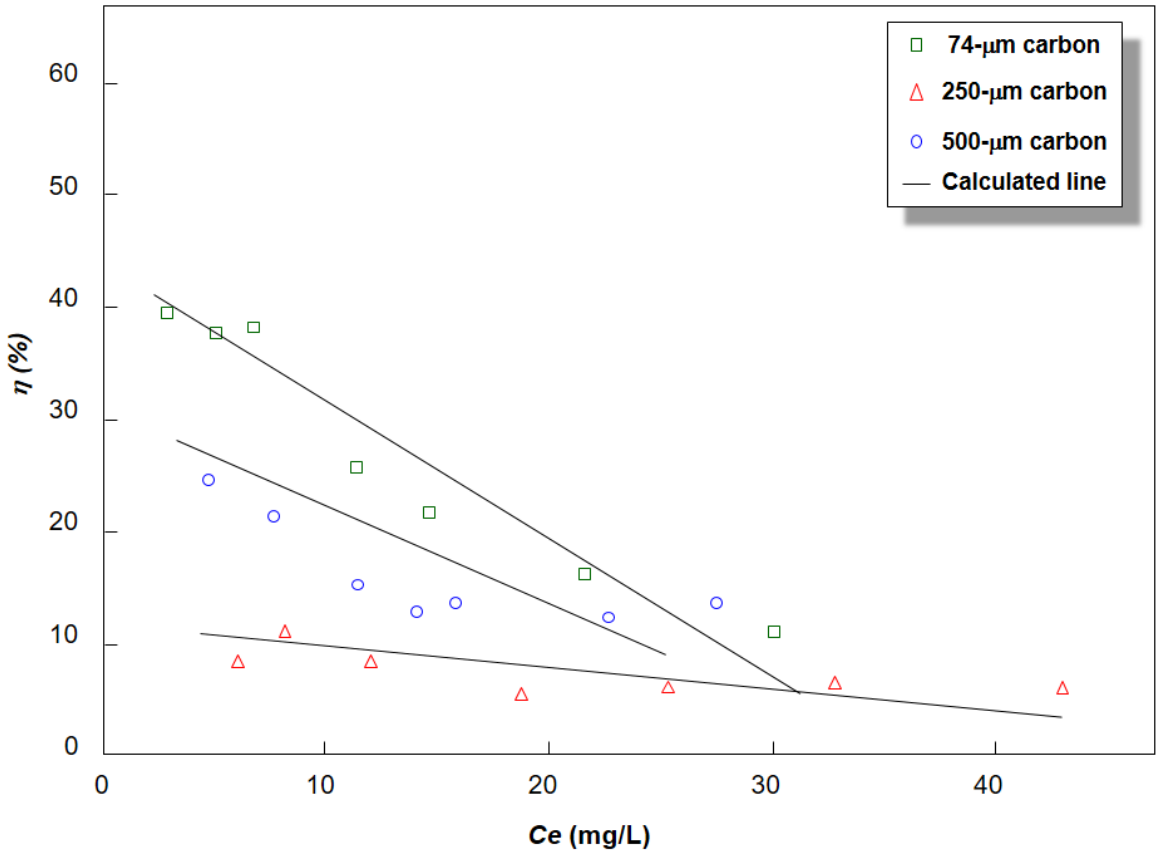

Figure 3. Comparison of experimental and predicted efficiency of adsorption of carbon microparticles.

Table 1 Isotherm models and their linear form. Table was adopted from reference[11]

Adsorption isotherm model	Initial equation	Linear form	Plot
Langmuir	$q_e = \frac{q_m.K_L.C_e}{1+K_L.C_e}$	$\frac{1}{q_e} = \frac{1}{q_m.K_L}\frac{1}{C_e} + \frac{1}{q_m}$	$\frac{1}{q_e}$ vs. $\frac{1}{C_e}$
Freundlich	$q_e = K_F.C_e^{1/n}$	$\ln q_e = \ln K_F + \frac{1}{n}\ln C_e$	$\ln q_e$ vs. $\ln C_e$
Temkin	$q_e = B_T(\ln A_T.C_e)$	$q_e = B_T(\ln C_e) + (B_T \ln A_T)$	q_e vs. $\ln C_e$
	$\theta = \frac{RT}{\Delta Q}\ln(K_T.C_e)$	$\theta = \frac{RT}{\Delta Q}\ln(C_e) + \frac{RT}{\Delta Q}\ln(K_T)$	θ vs. $\ln(C_e)$
Dubinin-Radushkevich	$\ln q_e = \ln q_s - \beta\varepsilon^2$	$\ln q_e = \ln q_s - \beta\varepsilon^2$	$\ln q_e$ vs. ε^2
Flory-Huggins	$\frac{\theta}{C_O} = K_{FH}(1-\theta)^{nFH}$	$\ln\left(\frac{\theta}{C_O}\right) = nFH\ln(1-\theta) + \ln K_{FH}$	$\ln\left(\frac{\theta}{C_O}\right)$ vs. $\ln(1-\theta)$
Fowler–Guggenheim	$K_{FG}.C_e = \frac{\theta}{1-\theta}\exp\left(\frac{2.\theta.W}{R.T}\right)$	$\ln\left(\frac{C_e(1-\theta)}{\theta}\right) = -\ln K_{FG} + \frac{2.\theta.W}{R.T}$	$\ln\left(\frac{C_e(1-\theta)}{\theta}\right)$ vs. θ
Hill-de Boer	$K_1.Ce = \frac{\theta}{1-\theta}\exp\left(\frac{\theta}{1-\theta} - \frac{K_2\theta}{RT}\right)$	$\ln\left(\frac{C_e(1-\theta)}{\theta}\right) - \frac{\theta}{1-\theta} = -\ln K_1 - \frac{K_2.\theta}{R.T}$	$\ln\left(\frac{C_e(1-\theta)}{\theta}\right) - \frac{\theta}{1-\theta}$ vs. θ

Plotting analysis result of Langmuir, Freundlich, Temkin, Dubinin-Radushkevich, Flory-Huggins, Fowler-Guggenheim and Hill-de Boer Model are presented in Figures 4 to 10, respectively. Detailed information for the parameter obtained from the plotting analysis shown is shown in Table 2.

Figure 4 shows the plotting analysis based on the Langmuir model. Plotting analysis showed that the carbon microparticles with sizes of 500 and 250 μm have R^2 values of 0.5424 and 0.7991, respectively, and that with smaller sizes (less than 74 um) have R^2 of more than 0.07. This informs that the adsorption process using the present carbon microparticles of less than 74 μm have the potential for the formation of monolayer structure. The maximum adsorption capacities as q_m of carbon particles increased when using smaller carbon sizes. The R_L analysis showed the values in the range of between 0 and 1 for all sizes, informing the characteristics of carbon microparticles in the favorable condition, in which the adsorption process can be controlled by changing process condition. Analysis of ΔGf informed that all processes were done spontaneously for all carbon sizes.

Figure 5 shows the plotting analysis based on the Freundlich model. Plotting analysis showed that the R^2 values of carbon particles with sizes of 500 μm and less than 250 μm were 0.22 and greater than 0.84, respectively. The values of R^2 in the Freundlich model for particles with sizes of less than 74 μm are the highest compared to that in the other models, informing that the adsorption profile of carbon microparticles with sizes of less than 74 μm fitted with the Freundlich model (having multilayer structure in the adsorption process). Analysis of n value for carbon microparticles showed the correlations of $n > 1$ and $1/n < 1$, giving results that adsorption occurs physically with a favorable process. However, for the case of particles with sizes of 250 μm, they have n value of less than 1. We also found that the cooperative process did not happen, informing that the multilayer is not due to the interaction between adsobate molecules.

Figure 6 is the plotting analysis results based on the Temkin model. R^2 values were varied. This model is good with enough R^2 values for carbon with sizes of 74 μm. However, for other sizes, the R^2 values were less than 0.85, informing that this model is not fit. The $ß_T$ values showed that the carbon microparticles with sizes of less than 74 μm involved chemical interaction, whearas carbon with larger sizes interfered physical interaction.

Figure 7 shows the plotting analysis based on the Dubinin-Radushkevich model. R^2 values for this model is the worst, informing that adsorption profile using carbon particles will not follow this model. Adsorption capacities q_s of the carbon particles are less than q_m gained from Langmuir model, in which the values cannot be guaranteed due to the less R^2 values. The analysis of E value in this model also confirmed that the process involved physical process for all cases.

Figure 8 shows the plotting analysis based on the Hill-de Boer model. R^2 values for this model is good for all particle sizes ($R^2 > 0.76$). This model is the most fitted model for particles with sizes of larger than 74 μm, informing the involvement of monolayer structure in the adsorption process. The values of K_2 confirmed that there is some attractions among the adsorbed molecules.

Figure 9 shows the plotting analysis based on Fowler-Guggenheim model. R^2 values for this model is good for all particle sizes ($R^2 > 0.75$). The analysis of W values showed that the adsorbed molecules repulse each other and involve an endothermic reaction. The values of Gibbs energy from this K_{FG} also presented negative values, informing the spontaneous adsorption process.

Figure 10 shows the plotting analysis based on the Flory-Huggins model. R^2 values for this model is less compared to other models. The analysis of number of molecules nFH confirmed the existence of interaction between adsorbed molecules and free molecules in the solution. The free molecules attached and interacted on the adsorbed molecules. The number of interacted

molecules increases with smaller carbon particle sizes. The values of the Gibbs free energy from this K_{FH} also presented negative values, informing the spontaneous adsorption process.

Table 2 Adsorption parameters based on standard isotherm models

Model	Parameter	Particle size (µm)			Notes
		500	250	74	
Langmuir	q_{max}(mg/g)	18.09	14.85	16.42	The maximum monolayer adsorption capacity
	K_L (L/mg)	0.3259	0.0928	0.0171	Langmuir adsorption constant
	R_L	0.1884	0.3696	0.6788	$0 < R_L < 1$, favorable adsorption.
	R^2	0.5424	0.7991	0.8727	The correlation coefficient.
	ΔGf (kJ/mol)	-34.53	-37.64	-41.83	$\Delta Gf < 0$, spontaneous process
Freundlich	n	8.6837	0.4795	1.4231	For 74 and 500 µm, $n < 1$, adsorption with chemical process
					For size 250 µm, $n > 1$, adsorption with physical process.
	$1/n$	0.1152	0.4795	0.7027	$1/n = 0 - 1$, favorable adsorption.
	k_f(mg/g)	10.6809	2.2553	0.4961	The Freundlich constant
	R^2	0.2277	0.8477	0.8927	The correlation coefficient.
	ΔGf (kJ/mol)	-25.88	-29.74	-33.49	$\Delta Gf < 0$, spontaneous process
Temkin	A_T (L/g)	3078.3121	0.4084	0.1808	The equilibrium binding constant
	β_T (J/mol)	1.3791	4.7317	3.5508	$\beta_T < 8$ kJ, physical adsorption
	R^2	0.1812	0.7646	0.8553	The correlation coefficient.
	KT	0.0100	0.0054	0.0011	The Temkin constant
	ΔGf (kJ/mol)	13.6638	28.1000	98.9960	$\Delta Gf > 0$, endothermic process
	R^2	0.9582	0.8630	0.5692	The correlation coefficient.
Dubinin-Radushkevich	q_s(mg/g)	16.48	11.22	6.99	The maximum adsorption capacity
	β (mol^2/kJ^2)	2.14	6.39	19.10	The Dubinin-Radushkevich isotherm saturation capacity
	E (kJ/mol)	0.4835	0.2797	0.1618	$E < 8$ kJ/mol, physical adsorption
	R^2	0.6640	0.5668	0.7577	The correlation coefficient
Hill-de Boer	K_1 (L/mg)	0.000791	0.000510	0.000175	Hill–de Boer constant
	K_2 (kJ/mol)	31.02	42.97	88.00	$K_2 > 0$, attraction between adsorbed molecules
	R^2	0.9914	0.9505	0.7560	The correlation coefficient

Fowler–Guggenheim	*W* (kJ/mol)	-12.60	-19.41	-42.47	*W* < 0, repulsion among adsorbed molecules and negative heat of adsorption
	K_{FG} (L/mg)	0.000985	0.000552	0.000177	Fowler–Guggenheim equilibrium constant
	R^2	0.9867	0.9396	0.7424	The correlation coefficient
Flory-Huggins	*nFH*	4	10	28	Number of adsorbates occupying on the surface site
	K_{FH} (L/mg)	0.001710	0.000827	0.000211	Flory-Huggins constant
	ΔGf (kJ/mol)	-15.79	-17.59	-20.97	*ΔGf*< 0, spontaneous process
	R^2	0.9587	0.9124	0.7109	The correlation coefficient

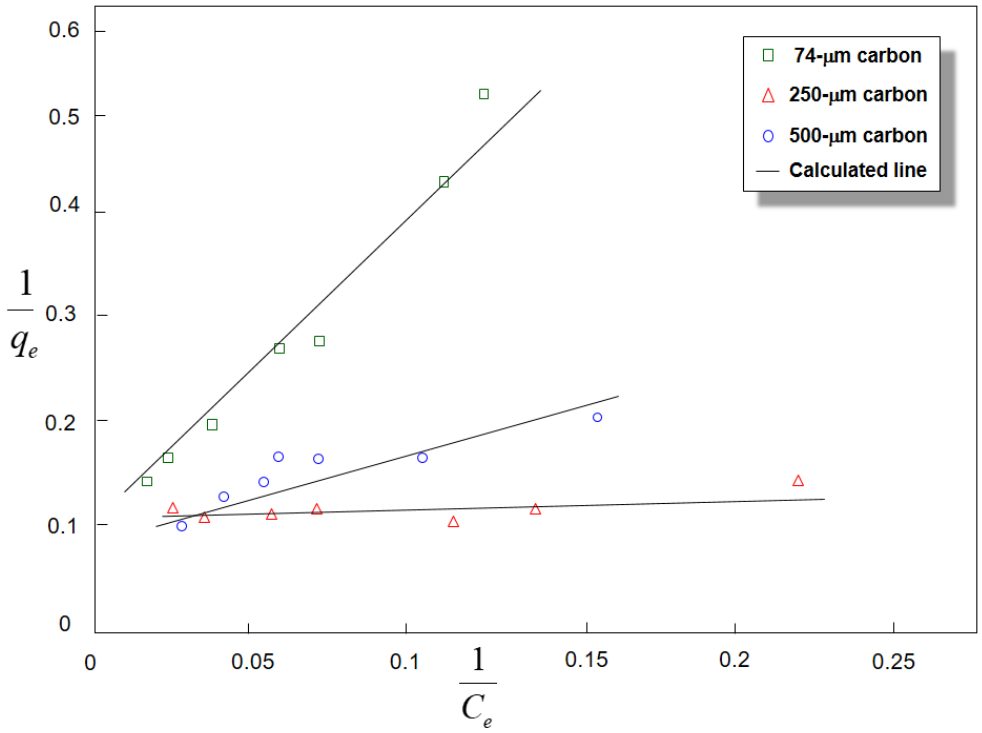

Figure 4. Langmuir adsorption isotherm of curcumin on various sizes of carbon microparticles.

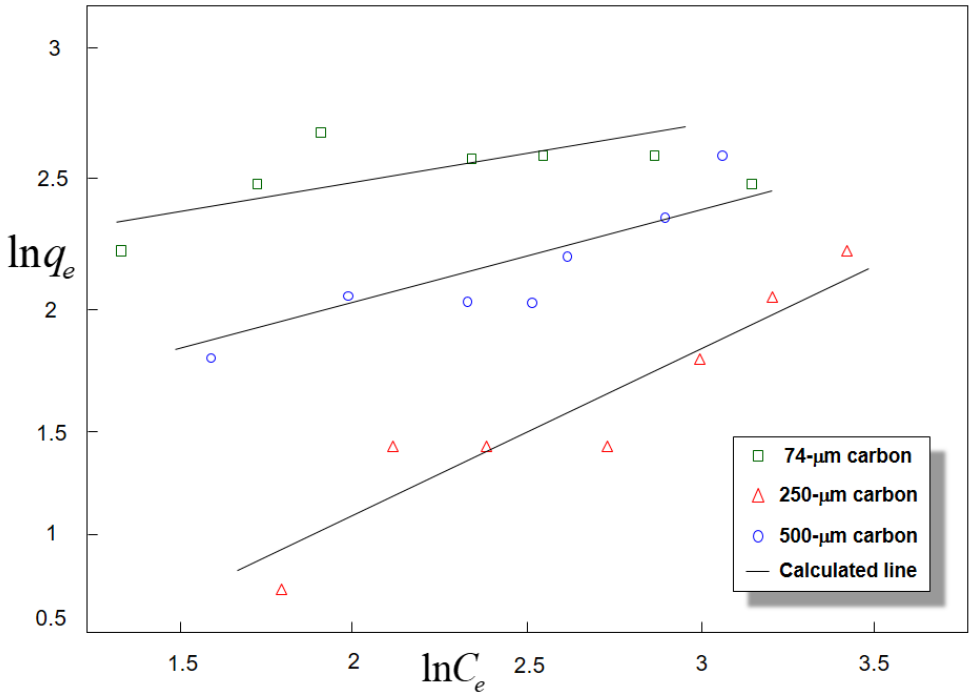

Figure 5. Freundlich adsorption isotherm of curcumin on various sizes of carbon microparticles.

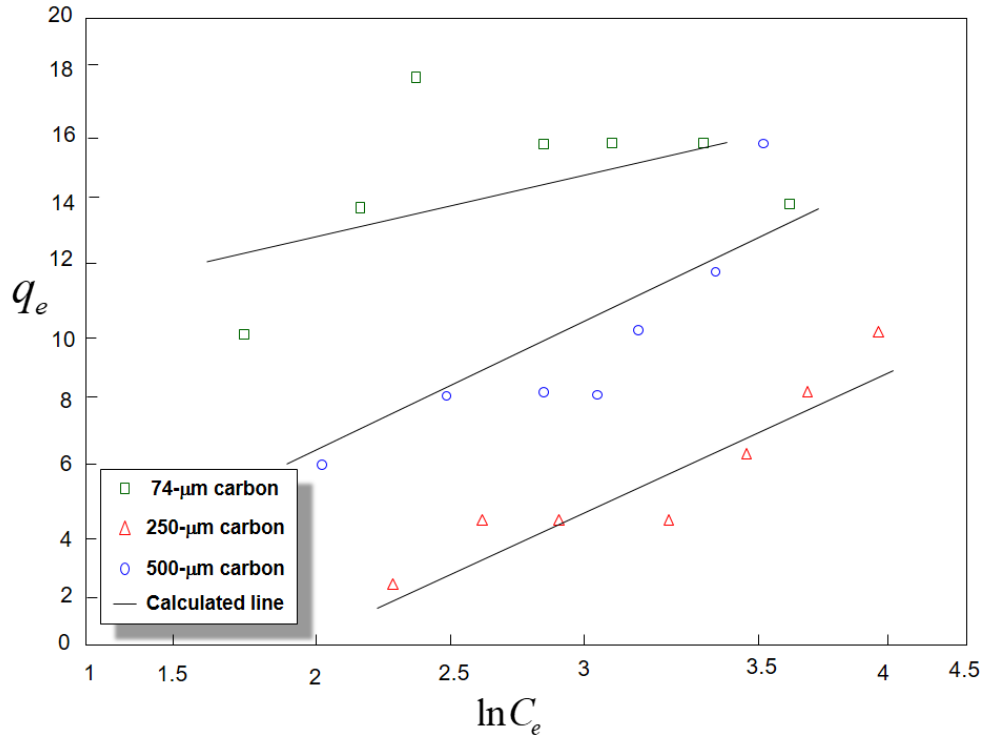

Figure 6. Temkin adsorption isotherm of curcumin on various sizes of carbon microparticles.

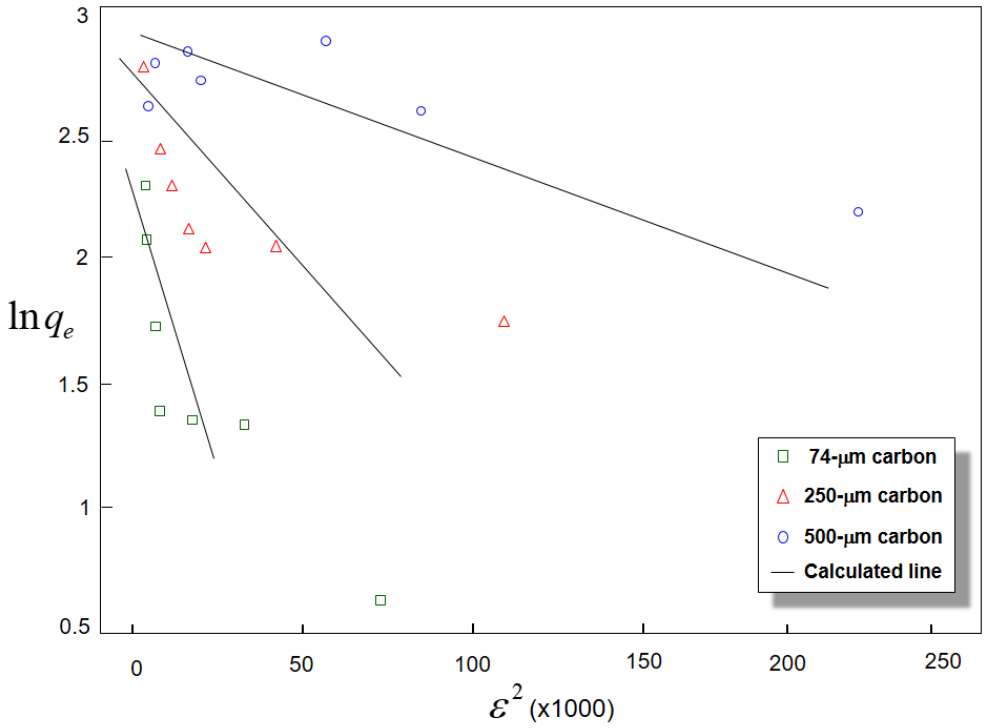

Figure 7. Dubinin-Radushkevich adsorption isotherm of curcumin on various sizes of carbon microparticles.

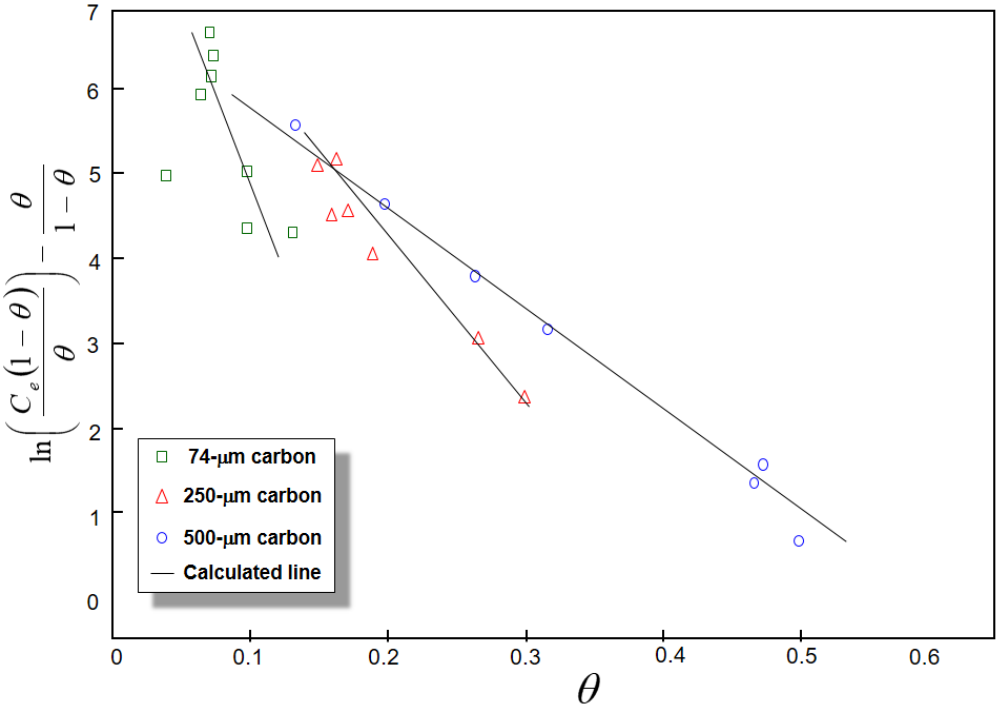

Figure 8. Hill-de Boer adsorption isotherm of curcumin on various sizes of carbon microparticles.

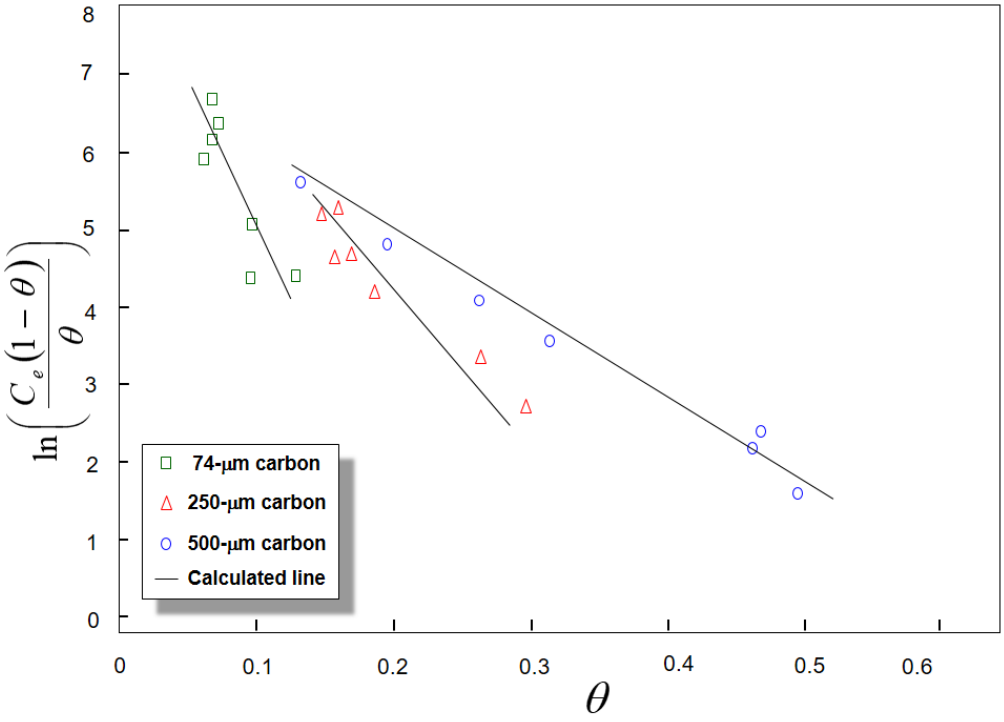

Figure 9. Fowler-Guggenheim adsorption isotherm of curcumin on various sizes of carbon microparticles.

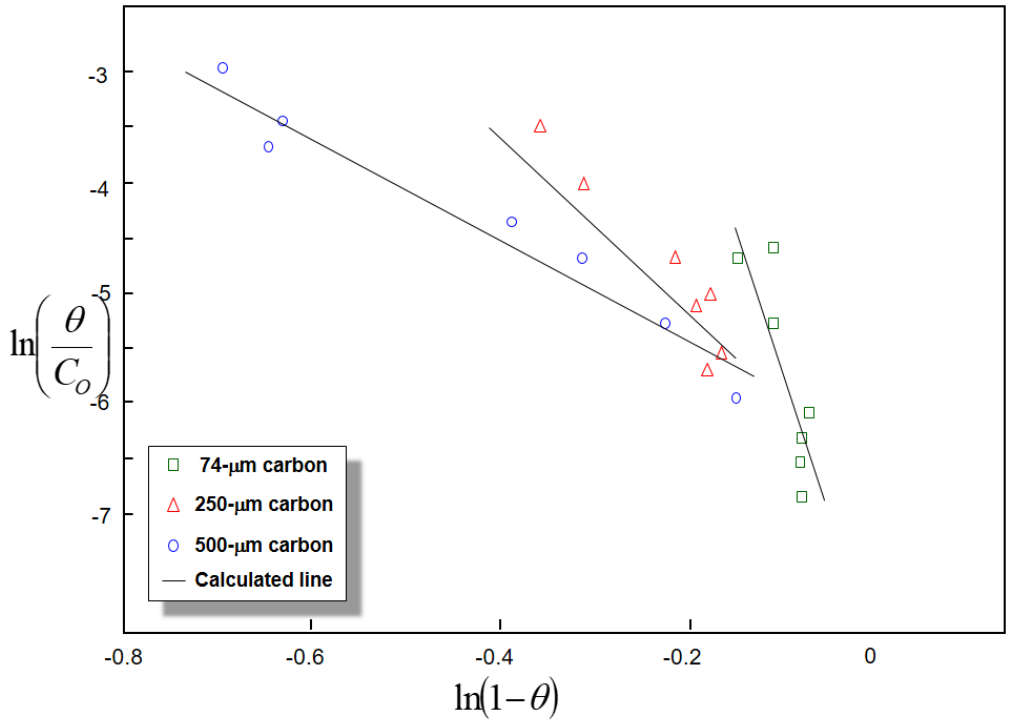

Figure 10. Flory-Huggins adsorption isotherm of curcumin on various sizes of carbon microparticles.

The adsorption analysis showed that the best isotherm model based on R^2 value from the linear fitting analysis was found in the Hill-de Boer isotherm model, which was closer to 1 (see Table 2). The data of Table 2 replied that the best fit isotherm models subsequently were Langmuir, Temkin, Freundlich, Dubinin-Radushkevich, Flory-Huggins, and Fowler–Guggenheim adsorption models. The detailed explanations for each model are discussed as follows.

The Langmuir isotherm adsorption model (see Figure 4) was found as the fifth best fit model in the fitting analysis. The Langmuir parameters, i.e. $q_{max,}$ K_L, R_L, and R^2 value, were investigated based on equations (2) and (3). Unlike Freundlich model, the adsorption of Langmuir model has been assumed to be ideal and irreversible, giving restriction only to the formation of monolayer. Based on the experimental data, R_L ranged between 0 and 1, implying the favorable adsorption, and this result was in a good line with the Freundlich model about favorability results.

The Freundlich isotherm model (see Figure 5) was the most appropriate model to describe the type adsorb curcumin molecules on carbon microparticles compared to other models. Freundlich parameter, including k_f, n, $1/n$, and R^2 values, analyzed based onequation (1). From the experiment, the value is $1/n$ followed by $0.1 < 1/n < 0.4$, indicating the preferred adsorption process (normal adsorption process). Experiments found that the k_f value is in the range $0 < k_f < 1$, implies favorable and discouraging adsorptiondesorption. A value of $1/n$ less than 1 indicates normal adsorption. The value of n obtained in this work is greaterof 1, inform the physical process support on adsorption

The parameter of Temkin model (i.e., A_T, β_T, and R^2) (see Figure 6) was studied using equation (5). Temkin assumed that the heat adsorption of all molecules in the layer decrease linearly, which was characterized by the uniform distribution of binding energies. The value R^2 of Temkin model obtained in this experiment was less than Hill-de Boer model. β_T value indicated that $\beta_T < 8$ kj/mol, indicating a physical adsorption (physisorption)

The Dubinin-Radushkevich isotherm model (see Figure 7) is used to the experimental data for determining the nature of the adsorption process. Linear fitting from Dubinin model was analyzed for obtaining q, E, R^2. The linear fitting analysis showed $E < 8$ kl/mol. The values of E for adsorption process using carbon particles having size of 75, 250, and 530 μm were obtained, indicating that the physical adsorption process is suitable for all sizes of carbon particles since the value of R is less than 8 kJ/mol.

The Hill-de Boer model (see Figure 8) already confirmed the results of analysis where $R^2 > 0.76$ for this model is good for all particles sizes. The values of K_2 ($K_2 > 0$) confirmed that there is some attraction among the adsorbed molecules. The particles with sizes of larger than 74 μm followed the Hill-de Boer model, confirming the monolayer structure and attraction in the adsorption process.

The Fowler–Guggenheim (see Figure 9) takes the lateral interaction of the adsorbed molecules during the adsorption process. Based on Table 2, the heat varies linearly with loading adsorbed molecules on the surface of adsorbent is $W < 0$, informing repulsion among adsorbed molecules and existence of endothermic processes and the values of Gibbs energy from this K_{FG} also presented negative values, informing the spontaneous adsorption process.

The Flory-Huggins isotherm model (see Figure 10) is occasionally used for understanding degree of surface coverage characteristics of adsorbate onto surface of adsorbent. The analysis of number of molecules *nFH* confirmed the existence of interaction between adsorbed molecules and free molecules in the solution. The free molecules attached and interacted on the adsorbed molecules. Based on Table 2, the number of interacted molecules increases with smaller carbon particle sizes. The values of the Gibbs free energy from this K_{FH} also presented negative values, informing the spontaneous adsorption process.

Based on above discussion, Hill-de Boer model is the best model in this study. The data of regression value in Table 2 indicated that the best fit isotherm models sequentially followed Hill-de Boer > Fowler > Flory >Temkin> Langmuir > Dubinin > Freundlich. Based on this model[11], the adsorption process takes place on a multilayer surface, and the adsorbent-adsorbate interaction is a physical adsorption (which confirmed and is good agreement with the results

from Hill-de Boer models and suitable with Freundlich, Temkin, and Dubinin-Radushkevich). Adsorption is carried out at different locations energetically under endothermic processes. The Gibbs free energy calculated is negative for all models, informing that the adsorption process is done spontaneously.

The results confirmed that the smaller sizes of adsorbents had a direct impact on the increase in adsorption capacity (due to the large surface area). Theoretically, the particle size of an adsorbent affects the adsorption performance. The adsorption capacity increases with decreasing particle size. Since adsorption is a surface phenomenon, it correlated to surface area and size of the adsorbents[10]. Surface area has an inverse relationship with particle size[26, 27]. As the surface area of the adsorbent particles increases, the particle size decreases, giving consequences in the increases in adsorption capacity (Q_{max}) and saturation capacity per unit mass of the adsorbent increases (Q_s). However, particles with smaller size (less than 250 μm) are less optimal in the adsorption process because of some aggregations between particles, making the particles larger. Indeed, further analysis must be done to confirm this aggregation phenomenon, such as electron microscope and nitrogen sorption analysis.

In addition, compared to other types of carbon particles in the similar sizes, the present carbon particles are relatively less ability in the adsorption. For example, previous study [11]showed that the carbon microparticles with sizes of 500, 200, and 100 μm prepared from pumpkin seeds have Qmax of 36.00; 35.15; and 38.68 mg/g, respectively. This is double value compared to the present carbon particles (see Table 1). The main reason is because the present carbon has less porosity. However, further analyses such as nitrogen sorption are required to confirm the structure of the particles.

4. CONCLUSION

Analysis of adsorption isotherm of carbon particles from soursop peel waste has been successfully done. This study concludes that seven isotherm models (i.e. Langmuir, Freundlich, Temkin, Dubinin-Radushkevich, Flory-Huggins, Fowler-Guggenheim, and Hill-de Boer isotherm models) provide good correlations for all particle size cases. Hill-de Boer model is the best model in this study. The adsorption process takes place on a multilayer surface, and the adsorbent-adsorbate interaction is a physical adsorption (which confirmed and is good agreement with the results from Hill-de bour models and suitable with Freundlich, Temkin, and Dubinin-Radushkevich). Adsorption is carried out at different locations energetically under endothermic processes. The Gibbs free energy calculated is negative for all models, informing that the adsorption process is done spontaneously.

ACKNOWLEDGEMENTS

We acknowledged Ristek Dikti (Penelitian Unggulan Perguruan Tinggi) and Bangdos Universitas Pendidikan Indoensia

REFERENCES

[1] Kurniawan, T.; Anwar, M.; Oktiani, R.; Ragadhita, R.; Nandiyanto, A.; & Aziz, M. Materials Physics & Mechanics **42**, 1 (2019) 151-157.
[2] Ratchahat, S.; Viriya-Empikul, N.; Faungnawakij, K.; Charinpanitkul, T.; & Soottitantawat, A. Science Journal Ubon Ratchathani University **1**, 2 (2010) 40-45.

[3] Akhtar, F.; Andersson, L.; Ogunwumi, S.; Hedin, N.; & Bergström, L. Journal of the European Ceramic Society **34**, 7 (2014) 1643-1666.
[4] Yorgun, S.; & Yıldız, D. Journal of the Taiwan Institute of Chemical Engineers **53**, (2015) 122-131.
[5] Kilic, M.; Apaydin-Varol, E.; & Pütün, A.E. Journal of Hazardous Materials **189**, 1-2 (2011) 397-403.
[6] Sych, N.; Trofymenko, S.; Poddubnaya, O.; Tsyba, M.; Sapsay, V.; Klymchuk, D.; & Puziy, A. Applied Surface Science **261** (2012) 75-82.
[7] Cazetta, A. L.; Vargas, A. M.; Nogami, E. M.; Kunita, M. H.; Guilherme, M. R.; Martins, A. C.; Silva, T. L.; Moraes, J. C.; & Almeida, V. C. Chemical Engineering Journal **174**, 1 (2011) 117-125.
[8] Rai, M.; Shahi, G.; Meena, V.; Meena, R.; Chakraborty, S.; Singh, R.; and Rai, B. Resource-Efficient Technologies **2** (2016) S63-S70.
[9] Moreno-Piraján, J.; & Giraldo, L. Journal of Analytical and Applied Pyrolysis **87**, 2 (2010) 188-193.
[10] Nandiyanto, A. B. D.; Girsang, G. C. S.; Maryanti, R.; Ragadhita, R.; Anggraeni, S.; Fauzi, F. M.; Sakinah, P.; Astuti, A.P.; Usdiyana, D.; and Fiandini, M. Communications in Science and Technology **5**, 1 (2020) 31-39.
[11] Nandiyanto, A. B. D. Moroccan Journal of Chemistry **8**, 3 (2020) 745-761.
[12] Nasri, N. S.; Hamza, U. D.; Ismail, S. N.; Ahmed, M. M.; & Mohsin, R. Journal of Cleaner Production **71**, (2014) 148-157.
[13] Kundu, A.; Gupta, B. S.; Hashim, M. A.; & Redzwan, G. Journal of cleaner production **105** (2015) 420-427.
[14] Fiandini, M.; Ragadhita, R.; Nandiyanto, A. B. D.; & Nugraha, W. C. Journal of Engineering Science and Technology **15**, 1 (2020) 022-031.
[15] Nandiyanto, A. B. D.; Putra, Z. A.; Andika, R.; Bilad, M. R.; Kurniawan, T.; Zulhijah, R.; & Hamidah, I. Journal of Engineering Science and Technology **12**, Special (2017) 1-11.
[16] Sukmafitri, A.; Ragadhita, R.; Nandiyanto, A.; Nugraha, W.; & Mulyanti, B. Journal of Engineering Science and Technology **15** (2020) 991-1000.
[17] Setyabudi, D. A.; & Broto, W. Studi Penempatan Lokasi dan Karakteristik Potensi Agroindustri Mangga dan Sirsak di Wilayah Jawa Barat. http://repository.pertanian.go.id/handle/123456789/3428, retrieved on August 15, 2020, vol, issue (2018).
[18] Sitepu, S.M.B. Strategi Pengembangan Agribisnis Sirsak di Kabupaten Deli Serdang (Studi Kasus Desa Durin Simbelang Kecamatan Pancur Batu). http://repositori.usu.ac.id/handle/123456789/2838, retrieved on August 15, 2020, vol, issue (2016).
[19] Yahya, M. A.; Mansor, M. H.; Zolkarnaini, W. A. A. W.; Rusli, N. S.; Aminuddin, A.; Mohamad, K.; Sabhan, F. A. M.; Atik, A. A. A.; & Ozair, L.N. AIP Conference Proceedings **1972**, 1 (2018) 030023.
[20] Nandiyanto, A. B. D.; Wiryani, A.; Rusli, A.; Purnamasari, A.; Abdullah, A.; Widiaty, I.; & Hurriyati, R. IOP Conference Series: Materials Science and Engineering **180**, 1 (2017) 012136.
[21] Hamdaoui, O.; & Naffrechoux, E. Journal of hazardous materials **147**, 1-2 (2007) 381-394.
[22] Saadi, R.; Saadi, Z.; Fazaeli, R.; & Fard, N.E. Korean Journal of Chemical Engineering **32**, 5 (2015) 787-799.

[23] Ali Fil, B.; Korkmaz, M.; & Özmetin, G. Journal of the Chilean Chemical Society **59**, 4 (2014) 2686-2691.
[24] Nandiyanto, A. B. D.; Andika, R.; Aziz, M.; & Riza, L.S. Indonesian Journal of Science and Technology **3**, 2 (2018) 82-94.
[25] Wachirasiri, P.; Julakarangka, S.; & Wanlapa, S. Songklanakarin Journal of Science & Technology **31**, 6 (2009) 605-611.
[26] Gultom, E. M.; & Lubis, M. T. Jurnal Teknik Kimia USU **3**, 1 (2014) 5-10.
[27] Haura, U.; Razi, F.; & Meilina, H. Biopropal Industri **8**, 1 (2017) 47-54.